INFECTION AND IMMUNITY, July 2011, p. 2510–2518 Vol. 79, No. 7
0019-9567/11/$12.00 doi:10.1128/IAI.00006-11

Contribution of Lethal Toxin and Edema Toxin to the Pathogenesis of Anthrax Meningitis▽

Celia M. Ebrahimi,[1] Tamsin R. Sheen,[1] Christian W. Renken,[2] Roberta A. Gottlieb,[1,3] and Kelly S. Doran[1]*

Department of Biology and Center for Microbial Sciences, San Diego State University, 5500 Campanile Dr., San Diego, California 92182[1]; Applied BioPhysics, Inc. Troy, New York 12180[2]; and BioScience Center, San Diego State University, 5500 Campanile Dr., San Diego, California 92182[3]

Received 4 January 2011/Returned for modification 7 February 2011/Accepted 14 April 2011

Bacillus anthracis **is a Gram-positive spore-forming bacterium that causes anthrax disease in humans and animals. Systemic infection is characterized by septicemia, toxemia, and meningitis, the main neurological complication associated with high mortality. We have shown previously that *B. anthracis* Sterne is capable of blood-brain barrier (BBB) penetration, establishing the classic signs of meningitis, and that infection is dependent on the expression of both major anthrax toxins, lethal toxin (LT) and edema toxin (ET). Here we further investigate the contribution of the individual toxins to BBB disruption using isogenic toxin mutants deficient in lethal factor, ΔLF, and edema factor, ΔEF. Acute infection with *B. anthracis* Sterne and the ΔLF mutant resulted in disruption of human brain microvascular endothelial cell (hBMEC) monolayer integrity and tight junction protein zona occludens-1, while the result for cells infected with the ΔEF mutant was similar to that for the noninfected control. A significant decrease in bacterial invasion of BBB endothelium *in vitro* was observed during infection with the ΔLF strain, suggesting a prominent role for LT in promoting BBB interaction. Further, treatment of hBMECs with purified LT or chemicals that mimic LT action on host signaling pathways rescued the hypoinvasive phenotype of the ΔLF mutant and resulted in increased bacterial uptake. We also observed that toxin expression reduced bacterial intracellular survival by inducing the bulk degradative autophagy pathway in host cells. Finally, in a murine model of anthrax meningitis, mice infected with the ΔLF mutant exhibited no mortality, brain bacterial load, or evidence of meningitis compared to mice infected with the parental or ΔEF strains.**

Bacterial penetration of the blood-brain barrier (BBB) results in meningitis and can develop into a life-threatening infection or be associated with permanent neurological sequelae. The BBB is composed of a specialized layer of human brain microvascular endothelial cells (hBMECs), which separates the brain and its surrounding tissues from the circulating blood and tightly regulates the flow of nutrients and molecules (6, 7). At the level of the microvasculature, brain endothelial cells are joined by tight junctions, which effectively limit the passage of substances except the smallest molecules (6, 7). Yet despite its highly restrictive nature, certain bacterial pathogens are still able to penetrate the BBB and gain entry into the central nervous system (CNS). Meningitis-causing bacteria interact with brain endothelium and can cross the BBB as live bacteria either transcellularly or paracellularly and subsequently multiply inside the CNS (29). The specific molecular and cellular mechanisms involved in this pathogen trafficking of brain endothelium may vary depending on the organism (29).

Bacillus anthracis, the etiologic agent of anthrax, is a Gram-positive spore-forming bacterium commonly found in the soil and can infect animals and humans (42). Anthrax is caused by ingestion, inhalation, or cutaneous inoculation of *B. anthracis* spores and their subsequent entry into host tissues (12). Spores germinate, multiply as vegetative bacteria, and disseminate throughout their host, causing septicemia, toxemia, and meningitis (12). Anthrax meningitis is characterized by an influx of neutrophil and monocytic cells, hemorrhage, edema, congestion of blood vessels, low cerebral spinal glucose levels, and the presence of bacteria in the cerebrospinal fluid (1, 19, 33). In general, even intensive antibiotic therapy is often ineffective against the rapid and lethal development of anthrax meningitis (33).

The pathogenicity of *B. anthracis* relies primarily on the major virulence factors, capsule and the toxin complexes. The anthrax toxins, encoded by genes on the major virulence plasmid, pXO1, are composed of three proteins, one receptor binding subunit, protective antigen (PA), and two catalytic subunits, lethal factor (LF) and edema factor (EF) (12, 43). PA forms a heptamer at the host cell membrane and binds to LF and/or EF, yielding lethal toxin (LT) and edema toxin (ET), respectively (15). The complex is then internalized and undergoes acidification, necessary for LF or EF translocation into the cytosol. Once in the cytosol, LF acts as a metalloprotease and cleaves members of the mitogen-activated protein kinase kinase (MAPKK) family, consequently disrupting signaling pathways (15, 59). EF is a Ca^{2+}- and calmodulin-dependent adenylate cyclase that generates high levels of cyclic AMP in the cell (36, 37) and contributes to virulence by inducing anti-inflammatory cytokines and suppressing lipopolysaccharide-mediated inflammatory tumor necrosis factor alpha release (25, 45). The coordinated action of both anthrax toxins ensures successful infection and overall virulence.

* Corresponding author. Mailing address: Department of Biology, College of Sciences, San Diego State University, 5500 Campanile Drive, San Diego, CA 92182-4614. Phone: (619) 594-1867. Fax: (619) 594-5676. E-mail: kdoran@sciences.sdsu.edu.

▽ Published ahead of print on 25 April 2011.

Central to the development of anthrax meningitis is the presence of bacilli in the CNS, suggesting the presence of factors that allow *B. anthracis* to traffic the BBB (1, 19). In order to identify these factors, we have previously developed *in vitro* and *in vivo* models of anthrax meningitis (58) and demonstrated that both anthrax toxins inhibit neutrophil signaling pathways and ultimately contribute to BBB penetration (58). However, the role of each individual toxin in the pathogenesis of meningitis has not been studied. Here we use isogenic bacterial mutants lacking EF or LF to examine the contribution of these toxins to BBB disruption, invasion, trafficking, and the development of meningitis during live bacterial infection. Our results suggest that both toxins contribute to BBB penetration in different ways but that LT plays a more prominent role in disease progression.

MATERIALS AND METHODS

Bacterial strains and growth conditions. *Bacillus anthracis* Sterne 7702 (pXO1 positive, pXO2 negative), the toxin mutant derivatives, and *Bacillus thuringiensis* (obtained from the Bacillus Genetic Stock Center, OH) were grown in brain heart infusion broth (BHI; Sigma) as shaking cultures under aerobic conditions at 37°C. Log-phase cultures of all strains were grown to an optical density at 600 nm of 0.4 (1×10^7 CFU/ml). The strain deficient in LF and EF toxins (ΔLF/EF) and mutants deficient in a single toxin (ΔLF and ΔEF) were generously provided by Scott Stibitz (Center for Biologics Evaluation and Research, Bethesda, MD) and described previously (27). The growth kinetics of all strains were similar in BHI and tissue culture medium under the experimental conditions used in our assays.

Endothelial cell culture and invasion assays. The human brain microvascular endothelial cell line, obtained from Kwang Sik Kim (Johns Hopkins University, Baltimore, MD), has been described previously (53, 54). hBMECs were cultured using RPMI 1640 (Gibco), supplemented with 10% fetal bovine serum (FBS; Gibco), 10% Nuserum serum replacement (BD Biosciences, San Jose, CA), and modified Eagle's medium nonessential amino acids (Gibco) without addition of antibiotics. Cultures were incubated at 37°C with 5% CO_2. Tissue culture flasks and 24-well plates were precoated with 1% rat tail collagen to support hBMEC monolayers.

B. anthracis Sterne and mutant strains were analyzed for their capacities to adhere to and invade hBMECs as described previously (13, 16, 58). Briefly, hBMECs were seeded in collagen-coated 24-well tissue culture plates until they reached 90 to 100% confluence. Early-log-phase bacteria were pelleted, washed with once phosphate-buffered saline (PBS), and diluted in RPMI 1640–10% FBS. An inoculum of 1×10^5 CFU/well (multiplicity of infection [MOI], 1 to 3) was added to hBMEC monolayers in a final volume of 500 μl, and plates were incubated at 37°C with 5% CO_2. To quantify the number of adherent organisms, hBMEC monolayers were incubated with bacteria for 45 min, washed five times with PBS to remove nonadherent bacteria, and disrupted by the addition of 0.025% trypsin–EDTA–Triton X-100 solution. To quantify intracellular bacteria, hBMEC monolayers were incubated with bacteria for 2 h, followed by the addition of gentamicin (50 μg/ml) for 15 min to kill extracellular bacteria. The monolayers were washed three times with PBS and disrupted by the addition of 0.025% trypsin–EDTA–Triton X-100 solution. Enumeration of adherent and intracellular organisms was performed by plating serial dilutions on Todd-Hewitt broth (THB; Sigma) agar plates. To quantify intracellular survival over time, intracellular bacteria were enumerated at the indicated time points after gentamicin treatment. Purified LF and PA were kindly provided by Stephen Leppla (National Institutes of Health, Bethesda, MD). Toxin proteins were diluted in sterile PBS, and hBMECs were incubated with 1 μg LF and 2 μg PA 30 min prior to infection. For MAP kinase assays, hBMECs were incubated with 10 μM UO126 (Sigma) or 10 μM SB202190 (Sigma) for 30 min prior to infection. All assays were performed at least in triplicate and repeated at least three times.

ECIS assays. The electric cell-substrate impedance-sensing (ECIS) system and electrode arrays (Applied BioPhysics, Inc., Troy, NY) were used to monitor monolayer integrity as described previously (35). hBMECs were grown on 30% collagen-coated 10-well electrode (8W10E) arrays until stable resistances of 800 Ω were reached. Confluent monolayers of hBMECs were infected with *B. anthracis* Sterne, ΔLF/EF, ΔLF, or ΔEF at an MOI of 0.1, and electrical resistances were recorded every 5 min for 12 h postinfection. Changes in transendothelial electrical resistance were then calculated according to the model of Giaever and Keese (20–22, 38). This method is based on noninvasive measurement of the frequency-dependent electrical impedance of cell-covered gold-film electrodes. The overall impedance of the system arises from three sources: the cell membrane capacitance (Cm), the resistance from the cell-electrode interaction (α), and the barrier function properties of the cell monolayer (Rb). Deconvolution of the overall ECIS signal into these parameters was performed by the ECIS software by fitting the mathematical model derived by Giaever and Keese (20) to the experimental data by least-squares optimization procedures. Once the barrier function of the cells is completely disrupted, the model is no longer valid, so loss of cells attached to the electrodes, i.e., cell monolayer integrity, was monitored by measurement of the reactance at 64 kHz (Fig. 1B). Controls were graphed as a function of the average producing a Rorschach ink blot. Duplicate samples were averaged.

ZO-1 staining. The hBMEC tight junction protein zona occludens-1 (ZO-1) was visualized following infection with *B. anthracis* Sterne or toxin-deficient mutants (1×10^6 CFU) as described previously (16). Following a 3- to 4-h incubation at 37°C, cells were washed three times with PBS, fixed in 4% paraformaldehyde, and permeabilized in 0.25% Triton-X. hBMECs were incubated in 2% goat serum, followed by incubation with 5 μg/ml anti-ZO-1 antibody (Invitrogen) overnight at 4°C. Cells were washed 3 times in PBS and then incubated with 5 μg/ml secondary antibody (Alexa Fluor 594-conjugated anti-rabbit). Slides were mounted in Vectashield mounting medium (Vector Laboratories) containing 4′,6-diamidino-2-phenylindole (DAPI), and images were digitally collected as stacks at a ×40 magnification on a Zeiss Axio Observer Z1 inverted microscope optimized for fluorescence equipped with a monochrome AxioCam MRm camera for imaging. Final images were produced using ImageJ software. Quantification of ZO-1 fluorescence was determined using the wavelet decomposition algorithm as we have described previously (16). The ZO-1 signal was represented as the number of bright pixels in our image and quantified in our program. Cell monolayer density was also quantified after infection by cell count.

Cytotoxicity assays. To quantify cytotoxicity, the concentration of lactate dehydrogenase (LDH) in cell culture medium was assayed with a CytoTox 96 nonradioactive cytotoxicity assay kit (Promega) according to the manufacturer's instructions.

GFP-LC3 imaging. To examine the autophagy response in hBMEC, cells were transfected with a green fluorescent protein (GFP)-tagged LC3 (26). At 24 h posttransfection, cells were incubated for 2 h with *B. anthracis* Sterne ΔLF/EF, ΔLF, or ΔEF mutants at an MOI of 10. Autophagosome induction was determined by quantifying GFP-LC3 punctae in a population of at least 200 cells. Cells were classified as either having diffuse GFP-LC3 fluorescence (0 to 30 GFP-LC3 dots/cell) or having numerous punctae GFP-LC3 structures (>30 GFP-LC3 dots/cell).

Mouse model of hematogenous meningitis. All animal experiments were approved by the Committee on the Use and Care of Animals at San Diego State University and performed using accepted veterinary standards. As described previously (16, 58), 9-week-old outbred immunocompetent female CD-1 mice (Charles River Laboratories, Wilmington, MA) were injected intravenously with 0.1 ml *B. anthracis* Sterne or a toxin-deficient mutant (1×10^6 CFU, $n = 6$ to 10 mice per group). Mice were monitored for signs of infection at least twice a day and euthanized when they became moribund. To assess the contribution of the toxins to BBB penetration, mice were euthanized at 43 h postinfection. Blood and brain and were collected and plated to determine bacterial counts in each tissue. Half of the brain was stored in 4% paraformaldehyde for further histology analysis, performed at the University of California, San Diego, Histopathology Core Facility (N. Varki, director). To quantify bacterial survival in whole mouse blood, blood was harvested from 9-week-old CD-1 mice. *B. anthracis* and the toxin-deficient mutants were incubated in whole mouse blood at 1×10^6 CFU/ml, and samples were taken at specific time intervals and serially diluted on THB agar to determine bacterial survival over time.

Statistical analysis. Graphpad Prism (version 4.03) software was used for statistical analysis. Differences in adherence, invasion, and bacterial counts in tissues were evaluated using an unpaired Student's *t* test. Statistical significance was accepted at *P* values of <0.05.

RESULTS

Edema toxin contributes to disruption of brain endothelium. Disruption of tight junctions and paracellular traversal between brain endothelial cells is one strategy employed by microbial pathogens to penetrate the BBB (29). As anthrax toxins have been implicated in promoting vascular permeabil-

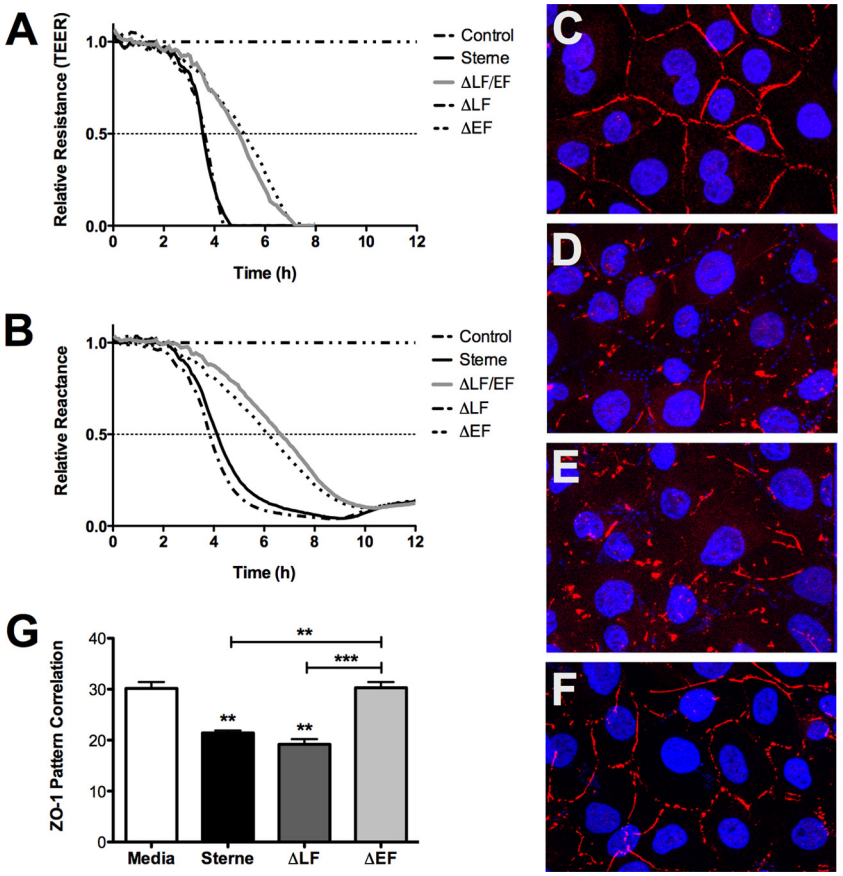

FIG. 1. EF contributes to decreased hBMEC barrier integrity and ZO-1 staining. ECIS measurements of TEER (A) and reactance (B). hBMECs were grown to confluence in ECIS arrays, and *B. anthracis* Sterne or isogenic toxin mutants were added to the monolayer at time zero. Impedance was recorded at 11 frequencies, and TEER was calculated as described in Materials and Methods. Cell viability and monolayer integrity were measured by the reactance at 64 kHz. Experiments were performed in duplicate, normalized to the mean for the control, and shown as means ± SEMs. (C to G) Tight junction ZO-1 staining in hBMECs. Immunofluorescence of ZO-1 and DAPI staining of monolayers incubated with cell culture medium, which served as the uninfected control (C), Sterne (D), ΔLF mutant (E), or ΔEF mutant (F). (G) ZO-1 fluorescence was quantified by pixel pattern correlation as described previously (16). Statistically significant differences are relative to the uninfected control. Error bars indicate 95% confidence intervals of mean values from three wells. **, $P < 0.005$; ***, $P < 0.001$.

ity (5, 9) and endothelial cell dysfunction (60), we sought to determine the contribution of LF and EF to hBMEC barrier integrity during infection by monitoring changes in transendothelial electrical resistance (TEER) across hBMECs and cell monolayer integrity (reactance) in real time by ECIS (Applied BioPhysics, Troy, NY). As described in Materials and Methods, hBMEC monolayers were seeded on electrode arrays until a stable resistance of 800 Ω was reached. Subsequent infection with *B. anthracis* Sterne or the ΔLF mutant resulted in a decrease in TEER to 50% of that for the uninfected control in ~3.5 h (Fig. 1A). A significant and marked delay in TEER reduction, with a mean time of 5 h until TEER is 50% of that of the control, was observed following infection with the ΔLF/EF or ΔEF mutants (Fig. 1A). This loss of TEER precedes the loss of cells attached to the electrode (as measured by reactance) by 16 to 30 min for the ΔLF mutant and *B. anthracis* Sterne, compared to 72 to 102 min for the ΔEF and ΔLF/EF mutants (Fig. 1B). This suggests that bacterial infection disrupts tight junction formation and barrier function prior to the eventual loss of cell monolayer integrity and that the EF toxin component promotes this disruption.

The protein ZO-1 is a primary regulatory protein of tight junction formation in the BBB (3, 10). To determine if the observed decrease in barrier integrity resulted from a disruption of hBMEC intercellular contacts, we quantified the expression and distribution of ZO-1 following infection with *B. anthracis* Sterne or the ΔLF or ΔEF mutant strains. Immunofluorescence staining showed an overall reduction and disruption of ZO-1 staining at the hBMEC intercellular junctions when cells were infected with *B. anthracis* Sterne or the ΔLF mutant compared to that observed in the medium control or during infection with the ΔEF strain (Fig. 1C to G). Further, we observed no difference in cell monolayer density during these infections (data not shown). Supernatants from these infections were also harvested to quantify cytotoxicity by LDH release, and no significant difference was observed following infection of all strains, suggesting that the differences in ZO-1 staining and barrier integrity were not a result of increased cell death (data not shown). Taken together these results suggest that during anthrax infection the EF toxin component contributes to ZO-1 and endothelial cell disruption.

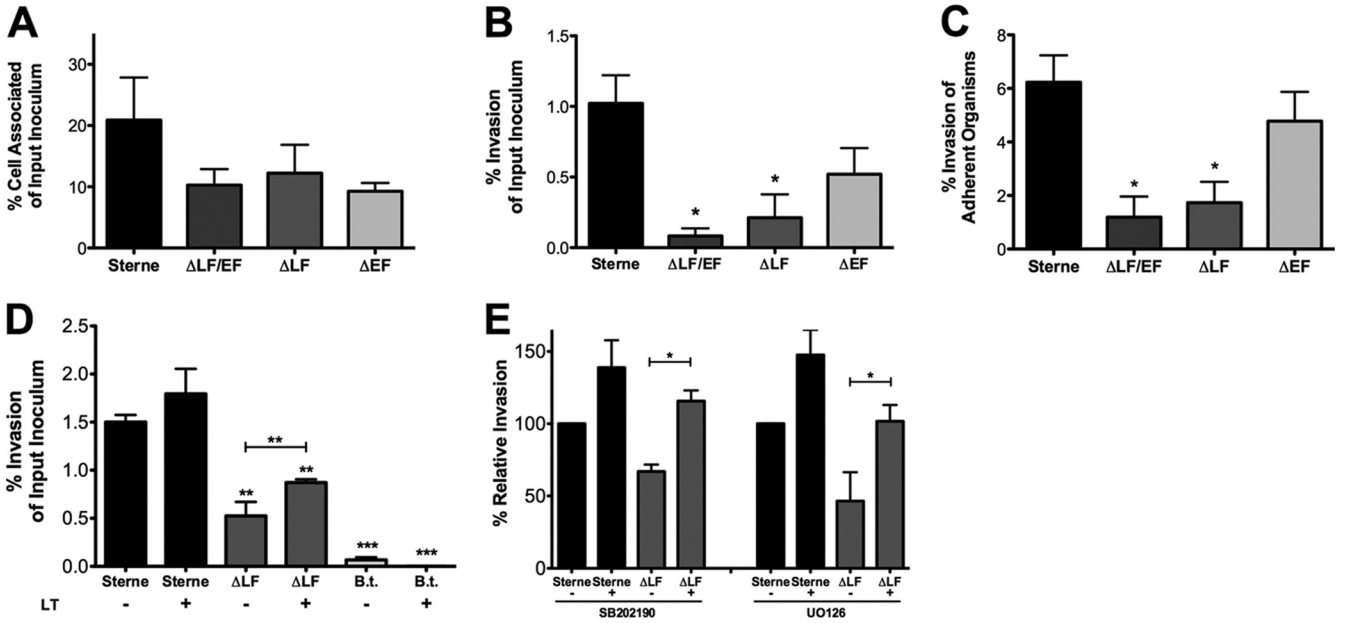

FIG. 2. LF contributes primarily to *B. anthracis* Sterne invasion of brain endothelium. Adherence to (A) and invasion of (B) hBMECs by *B. anthracis* Sterne and the isogenic ΔLF/EF, ΔLF, and ΔEF mutants. Data are expressed as the total number of cell-associated or intracellular CFU recovered compared to the input inoculum (at an MOI of $1 = \sim 1 \times 10^5$). (C) Level of adherent organisms that successfully invaded. Data are expressed as the percentage of invasive CFU recovered compared to the total number of cell-associated bacteria recovered for *B. anthracis* Sterne and the ΔLF/EF, ΔLF, and ΔEF mutants. (D) Percent invasion of hBMECs by *B. anthracis* Sterne and the ΔLF mutant in LT-treated and nontreated hBMECs. Statistically significant differences are relative to infection with the Sterne strain. Error bars indicated 95% confidence intervals of mean values from three separate experiments. B.t., *B. thuringiensis*. (E) Percent *B. anthracis* Sterne and ΔLF mutant intracellular CFU in MEK1/2 or p38 inhibitor-treated hBMECs relative to the number of dimethyl sulfoxide-treated cells. Experiments were performed in triplicate, normalized to the mean obtained using the Sterne strain, and shown as the mean ± SEM. Error bars indicate 95% confidence intervals of mean values from three experiments. *, $P < 0.05$; **, $P < 0.005$; ***, $P < 0.001$.

Lethal toxin promotes invasion of brain endothelium. The ability of meningeal pathogens to directly enter or invade brain endothelium and pass through the BBB transcellularly represents another strategy for breaching the BBB during the development of bacterial meningitis (29). We have previously shown that *B. anthracis* Sterne is able to adhere to, directly invade, and transmigrate through brain endothelium and that this effect is partially dependent on the anthrax toxins (58). We next sought to determine the contribution of individual toxin components, LF and EF, in mediating *B. anthracis* Sterne adherence and invasion of BBB endothelium *in vitro*. hBMECs were grown to confluence and infected with *B. anthracis* Sterne, ΔLF/EF, ΔLF, or ΔEF strains. Data are expressed as the percentage of adherent or intracellular CFU recovered compared to the initial input inoculum. No significant difference in adherence was observed between the strains (Fig. 2A); however, infection with ΔLF/EF or ΔLF mutants resulted in a marked decrease in the number of invasive CFU compared to the number of *B. anthracis* Sterne or ΔEF mutant invasive CFU (Fig. 2B). When the percentages of adherent organisms that subsequently go on to invade hBMEC were compared, we observed a reduced level of invasion of the adherent population during infection with the ΔLF/EF (1.2%) and ΔLF (1.7%) mutants compared to that during infection with *B. anthracis* Sterne (6.23%) and the ΔEF mutant (4.8%) (Fig. 2C). To further demonstrate the contribution of LT in promoting *B. anthracis* Sterne invasion, we pretreated confluent monolayers of hBMECs with purified LT and quantified the percent invasion of *B. anthracis* Sterne and the ΔLF mutant. A significant increase in ΔLF invasion was observed when hBMECs were pretreated with LT compared to untreated hBMECs (Fig. 2D). This increase in invasion was specific to *B. anthracis* Sterne, as the noninvasive bacterium *B. thuringiensis* did not exhibit an increase in invasion in the presence of LT. These results demonstrate that LF plays a specific role in facilitating *B. anthracis* Sterne hBMEC invasion.

Once it is translocated into cells, LF has been shown to cleave MEKs 1 through 7 (except MEK5) disrupting the activation of the MAPK pathways via extracellular signal-regulated kinase 1 (ERK1), ERK2, p38, and c-Jun N-terminal kinase (JNK) (4, 15). We hypothesized that disruption of the MAPK pathways by LT may modulate bacterial uptake, resulting in increased bacterial invasion. Previous studies with other cell types have shown that the action of LT can be replicated by treating cells with MEK and MAPK inhibitors (2, 31, 34, 60, 61). In addition, inhibition of MEK1/2 (upstream activator of ERK1/2) and p38 has been shown to induce lung endothelial barrier dysfunction similar to what is observed during treatment with LT (60). To examine whether inhibition of MAPK pathways can affect *B. anthracis* Sterne invasion, hBMECs were pretreated with a potent inhibitor of MEK1/2 (UO126) or p38 (SB202190) prior to the addition of bacteria. Both *B. anthracis* Sterne and the ΔLF mutant exhibited an increase in invasion following hBMEC pretreatment with UO126 or SB202190 (Fig. 2E), suggesting that inhibitors of the MAPK pathway mimic the action of LT to enhance bacterial uptake.

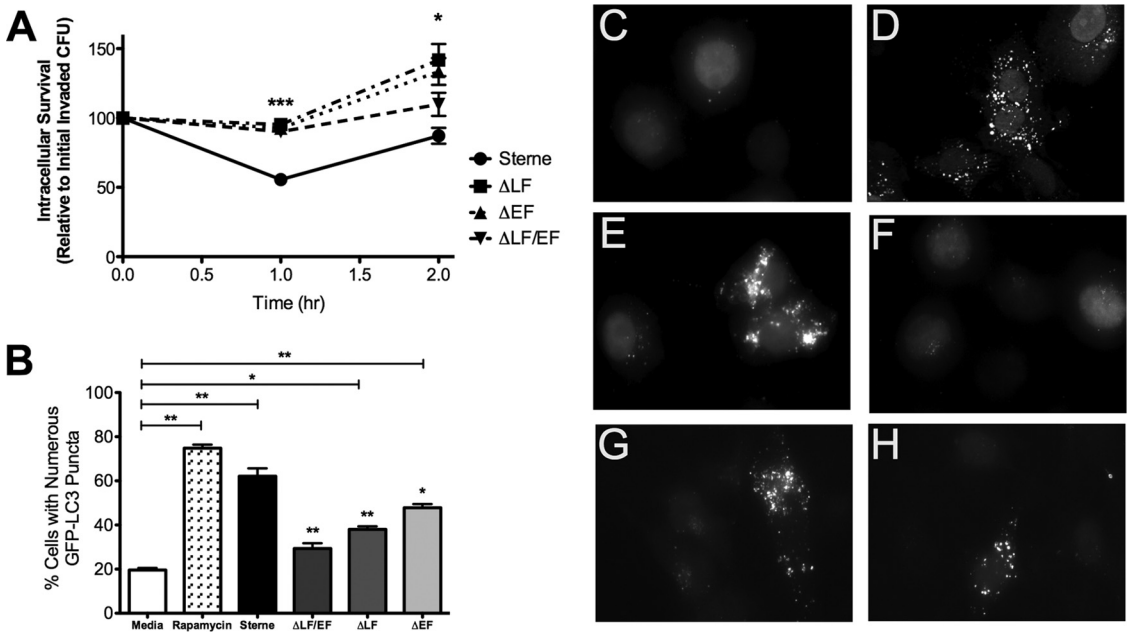

FIG. 3. LF and EF promote decrease in *B. anthracis* Sterne survival in hBMECs. (A) Survival of *B. anthracis* Sterne, ΔLF/EF, ΔLF, and ΔEF in hBMECs. (B) Quantification of GFP-LC3 puncta. Data from a representative experiment are shown; error bars indicate 95% confidence intervals of mean values from at least three wells. (C to H) GFP-LC3 distribution in hBMECs. GFP-LC3 puncta were quantified from hBMECs treated for 2 h with culture medium (C), 5 μM rapamycin (D), *B. anthracis* Sterne (E), ΔLF/EF mutant (F), ΔLF mutant (G), or ΔEF mutant (H). *, $P < 0.05$; **, $P < 0.005$; ***, $P < 0.001$.

Anthrax toxins affect intracellular survival and induce autophagy. Following bacterial invasion, intracellular survival of bacteria within brain endothelial cells is required for subsequent transcytosis and traversal of the BBB. To assess whether toxin production contributes to intracellular survival after bacterial entry, we performed a modified invasion assay in which the intracellular bacteria were quantified at different time points after addition of antibiotics to kill extracellular organisms. Following a 2-h infection with *B. anthracis* Sterne, ΔLF/EF, ΔLF, or ΔEF strains, the intracellular CFU were enumerated at 15 min and 1 and 2 h after antibiotic treatment. Data are expressed as the number of recovered intracellular CFU relative to that recovered following the 2-h invasion time after the 15-min antibiotic treatment (referred to as time zero). The numbers of recovered intracellular CFU remained relatively constant during infection with the ΔLF/EF, ΔLF, or ΔEF strains compared to those during infection with *B. anthracis* Sterne, which exhibited a significant decrease in intracellular organisms at 1 and 2 h postinfection (Fig. 3A). These results suggest that toxin expression may limit *B. anthracis* survival within hBMECs.

To survive intracellularly, bacteria must employ various strategies to resist the host cell defense system, including resistance to phagolysosome and autophagic killing. Our observation prompted us to examine the bulk degradative autophagic pathway which can be induced during microbial infection as a mechanism to eliminate intracellular pathogens and/or toxins (11). Autophagy is a physiologic process whereby cytoplasmic components, including organelles and intracellular microbes, are engulfed by a double membrane structure and targeted for destruction by fusion with a lysosome. Upon initiation of autophagy, the cytosolic LC3-I form is converted to the LC3-II form, which is covalently linked to phospholipids and associated with autophagosomal membranes (28). When GFP is fused to the N terminus of LC3, the GFP-LC3 is diffusely distributed in the cytosol, but upon proteolysis of the C terminus and lipidation, it is recruited into autophagosomes, which are evident as microscopic specks, or punctae. The extent to which GFP-LC3 is recruited into punctate structures correlates very well with the extent of autophagy and is now regarded as a reliable indicator of autophagy (24, 26, 48, 55).

Recently, it was shown that intoxication of macrophages with purified LT induced autophagy, suggesting that autophagy functions as a defense mechanism against LT-mediated toxemia (55). To investigate whether autophagy is induced in hBMECs in response to toxin production during infection with live bacteria, we monitored and quantified GFP-LC3 puncta following a 2-h infection with *B. anthracis* Sterne or the toxin-deficient mutants. A significant increase in the percentage of hBMECs with high numbers of GFP-LC3 punctae was observed when they were infected with *B. anthracis* Sterne compared to the ΔLF/EF, ΔLF, and ΔEF strains or the uninfected control (Fig. 3B to H). Of note, under the conditions tested in this assay, we observed no significant difference in LDH release in hBMECs during infection with the parental and mutant strains (data not shown). These results demonstrate that the observed increase in autophagy during *B. anthracis* infection is mediated by both toxin complexes. This finding is consistent with the observed decrease in the number of *B. anthracis* Sterne intracellular CFU, suggesting that intracellular *B.*

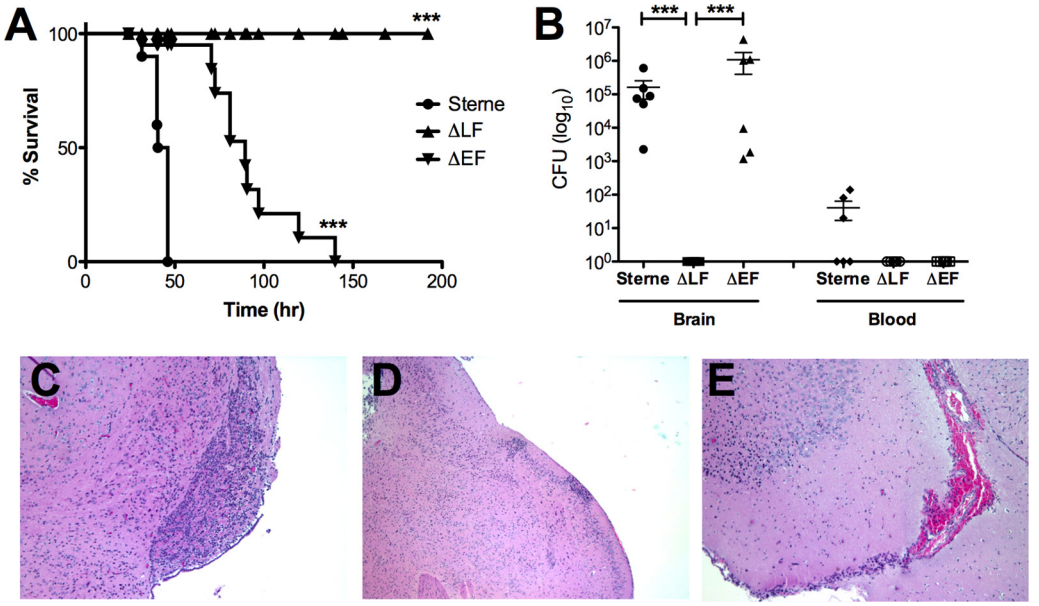

FIG. 4. Contribution of LF and EF to development of anthrax meningitis. (A) Kaplan-Meier survival curve of CD-1 mice upon infection with *B. anthracis* Sterne, ΔLF, or ΔEF. Mice were injected intravenously with 1×10^6 CFU of bacteria, and survival was monitored at least twice a day over a 4-week period. (B) LF contributes to BBB penetration *in vivo*. Bacterial counts from the blood and brains of CD-1 mice 43 h after intravenous infection with 1×10^6 CFU of *B. anthracis* Sterne, ΔLF mutant, or ΔEF mutant. Lines represent mean numbers of bacterial CFU. Experiments were performed at least twice, and results of a representative experiment are shown. (C and E) Histopathology of hematoxylin-and-eosin-stained brain tissues of representative individual mice infected with *B. anthracis* Sterne (C) showing meningeal thickening and cellular infiltration. (D) Brain of a mouse infected with the ΔLF mutant showing normal meningeal pathology with some cellular infiltration. (E) Brain of a mouse infected with ΔEF showing meningeal inflammation, cellular infiltration, and hemorrhage. *, $P < 0.05$; ***, $P < 0.001$.

anthracis Sterne is targeted to the autophagic pathway at early stages of infection.

Contribution of anthrax toxins to development of meningitis. Our results thus far suggest that both anthrax toxins contribute to different aspects of BBB disruption and penetration *in vitro*. We hypothesized that these *in vitro* phenotypes would translate into a diminished ability to penetrate the BBB and produce meningitis *in vivo*. Using our established murine model of hematogenous anthrax meningitis (58), we infected mice intravenously with *B. anthracis* Sterne, ΔLF, or ΔEF strains ($n = 10$ per group). Infection with *B. anthracis* Sterne resulted in complete mortality, while all of the ΔLF-infected mice survived (Fig. 4A). Interestingly, mice infected with the ΔEF mutant exhibited a significant delay in mortality of 2 to 5 days postinfection ($P < 0.0001$; Fig. 4A). In subsequent experiments, mice were similarly infected ($n = 6$ per group) and euthanized at 43 h postinfection, after which time blood and brain and were harvested from each mouse for quantitative bacterial culture and histopathologic analysis. All mice infected with *B. anthracis* Sterne or the ΔEF mutant had statistically significantly higher bacterial counts in the brain, while no bacteria were recovered from the brains of mice infected with the ΔLF mutant (Fig. 4B). No difference in the number of CFU in the blood was observed between the strains at the time that tissues were harvested (Fig. 4B). Additionally, we observed no significant difference in mouse whole-blood survival assays performed *ex vivo* between *B. anthracis* Sterne and the toxin-deficient mutants (data not shown). Microscopic examination of the brain tissues from representative mice infected with *B. anthracis* Sterne or the ΔEF mutant showed an influx of inflammatory cells and substantial hemorrhaging (Fig. 4C and E), whereas the brains of mice from infected ΔLF mice exhibited normal brain architecture (Fig. 4D). These results suggest that the LT complex plays a more prominent role in facilitating BBB penetration and the development of meningitis *in vivo*.

DISCUSSION

Previous studies have demonstrated the important contributions of anthrax toxins to the development of disease pathogenesis (18, 39–41). In this study, we used isogenic ΔLF and ΔEF mutants to characterize the contribution of the individual anthrax toxins, LT and ET, to BBB disruption, invasion, trafficking, and the development of anthrax meningitis in the context of a live bacterial challenge. Our results suggest a distinct role for ET in modulating brain endothelial integrity by disrupting the intercellular contacts and one for LT in promoting both invasion and penetration of the BBB, leading to colonization of the CNS. Both toxins were shown to induce the autophagy response in hBMECs that may act initially to limit intracellular growth of the pathogen. The results presented in this study demonstrate that both toxins contribute to virulence and BBB penetration but that LT plays a more prominent role in anthrax disease progression.

The endothelial barrier is a structural and functional barrier that protects the brain from microorganisms and toxins circulating in the blood (29). Pathogenic microorganisms have exploited several mechanisms to penetrate through host cell barriers, including disrupting the integrity of the cellular barriers through the action of secreted bacterial toxins (14, 16, 32, 35,

49, 52, 58, 60). Many aspects of anthrax disease can be attributed to the secretion of the anthrax toxins ET and LT. Purified preparations of LT have been shown to induce vascular collapse and subsequent hypoxia-mediated toxicity in mice (39) and disrupt lung endothelial and epithelial barrier integrity (34, 60) but do not account for renal dysfunction and hemorrhage of the gastrointestinal tract, lymph nodes, or meninges (18). The contribution of ET to anthrax disease is less clear, since obtaining significant quantities of recombinant ET has been difficult (18). In the present study we found that in the context of a live bacterial challenge, disruption of both barrier function and ZO-1 distribution was mediated primarily by ET and not LT. These results may differ from the previously reported results mentioned above because our studies primarily utilized live organisms as opposed to purified toxins. However, our results are consistent with those of recent studies using bacterial infection and purified ET toxin, where ET was found to contribute to disruption of the endothelial barrier *in vitro*, as measured by permeability to Evans blue dye, and to vascular effusion and pulmonary edema *in vivo* (23). Overall, our results suggest a principle role for ET in disruption of the integrity of the BBB endothelium.

Transcellular traversal of the BBB has been demonstrated for most meningitis-causing bacteria, such as *Streptococcus agalactiae* (44), *Escherichia coli* (30), *Staphylococcus aureus* (51), *Streptococcus pneumoniae* (50), and *B. anthracis* (58). Successful traversal of the BBB requires a pathogen to adhere, invade, and survive within brain endothelial cells. In the present study, we observed a marked decrease in invasion with the ΔLF isogenic mutant and that pretreatment of hBMECs with purified LT or chemical inhibitors of MAPK signaling pathways restored invasion levels close to those of the parent *B. anthracis* Sterne strain. This effect was specific, as LT did not induce uptake of the normally noninvasive but related strain *Bacillus thuringiensis*. Thus, our results suggest that LT activity promotes *B. anthracis* Sterne invasion. Although the mechanism is not entirely clear, it likely involves the MAPK signaling pathway. Modulation of this pathway has been shown to contribute to the invasive ability of other bacterial pathogens such as *Pseudomonas aeruginosa* (17), *Listeria monocytogenes* (56), and *Chlamydia pneumoniae* (8). In addition, it has been speculated that LT affects the integrity of host cell barriers by promoting expulsion of single senescent cells from the monolayer and hindering cytoskeletal repair through MAPK inhibition rather than disrupting tight junctions or producing massive cell death (34). This expulsion may result in the exposure of host cell surface receptors that promote bacterial invasion, as is seen with *L. monocytogenes* (46). Whether or not this mechanism is operating during *B. anthracis* invasion of BBB endothelium, as well as the identification of a host cell receptor(s), requires further investigation.

Successful traversal across host cell barriers requires the pathogen to survive within host cells. *B. anthracis* Sterne has been shown to penetrate the BBB *in vivo*, and expression of the anthrax toxins was essential for this transmigration (58). In this study, we assessed the ability of *B. anthracis* Sterne to survive within hBMECs and the contribution of the toxins to this effect. We observed a significant decrease in the numbers of intracellular CFU during the early stages of *B. anthracis* Sterne infection, followed by an increase in the numbers of the intracellular CFU at later time points. The decrease in the numbers of intracellular CFU was dependent on the expression of the anthrax toxins, since infection of hBMECs with either ΔLF or ΔEF mutant strains resulted in a relatively constant intracellular bacterial pool. These results demonstrate that intracellular survival of *B. anthracis* Sterne within the brain endothelium may be affected by toxin expression.

During bacterial infection, host cells can invoke autophagy as a mechanism to eliminate intracellular pathogens and/or toxins; however, this process can also be exploited by microbes for survival and replication and can lead to host cell death (11). Recent studies have shown the induction of autophagy by host cells in response to secreted toxins from *Vibrio cholerae* (24), *Helicobacter pylori* (57), and *B. anthracis* (55) presumably to enhance cytoplasmic clearing by diverting toxins to the autophagosome, where they are then degraded after subsequent lysosomal fusion. In the present work, we investigated whether autophagy was invoked by hMBECs in response to the toxins secreted during bacterial infection and whether this induction limited the intracellular survival of *B. anthracis* Sterne within hBMECs. Using live bacteria, we demonstrated that *B. anthracis* Sterne infection induced autophagy in brain endothelial cells in a toxin-dependent manner. Our results further suggest that the induction of autophagy during *B. anthracis* Sterne infection may function as a cellular defense mechanism leading to a decrease in the intracellular population of *B. anthracis* Sterne during the early stages of infection. However, at later time points, *B. anthracis* Sterne is able to either avoid or utilize the autophagic process, resulting in an increase in the intracellular pool. These findings are in line with the mechanism proposed for *L. monocytogenes*, where autophagy impaired intracellular growth during the early stages of infection but at later time points bacteria were able to evade autophagic surveillance, resulting in an increase in intracellular growth (48).

We have previously shown that development of anthrax meningitis is dependent on the expression of both anthrax toxins (58). We next sought to determine the contribution of each toxin to virulence by injecting mice with vegetative isogenic toxin mutants and monitoring survival. Our results demonstrate that LT is the primary virulence factor; however, ET was also less efficient at inducing mortality, suggesting a role for the adenylate cyclase during lethal infection. These results are in agreement with those obtained using spores injected subcutaneously into mice. Spores of isogenic strains of *B. anthracis* lacking LF or EF exhibited reduced virulence in a murine model compared to the wild-type strain, suggesting that both factors contribute to the disease process (47). Here we assessed the contribution of each toxin to BBB penetration *in vivo* during systemic infection of vegetative organisms by killing all infected mice at 43 h postinfection and determining dissemination to the brain. A complete absence of CFU was observed in mice infected with the ΔLF strain, whereas mice infected with *B. anthracis* Sterne or the ΔEF mutant exhibited high CFU numbers. Microscopic analysis of brain sections revealed that mice infected with ΔLF exhibited a normal brain architecture compared to that of mice infected with *B. anthracis* Sterne or ΔEF, which exhibited hemorrhaging and an influx of inflammatory cells. These results suggest that LT is the key virulence factor that promotes *B. anthracis* Sterne penetration of the BBB into the CNS.

In summary, our study determines the contribution of the anthrax toxins to the pathogenesis of anthrax meningitis and provides further insight into how these toxins function in the context of the vegetative organism. We demonstrate a role for ET in disrupting the barrier function of the BBB and a role for LT in promoting *B. anthracis* Sterne invasion and BBB penetration. Both toxins appear to limit *B. anthracis* Sterne intracellular survival during the initial phase of infection through the induction of autophagy; however, at later time points, *B. anthracis* Sterne was able to overcome this host cell defense mechanism. Finally, we show that both toxins contribute to overall survival in a murine model of infection but that LT and its role in promoting bacterial uptake play a more prominent role in ultimate BBB penetration and the development of meningitis. Our results suggest that LT may prove to be an attractive target for therapeutic intervention during anthrax disease.

ACKNOWLEDGMENTS

We are grateful to Monique Stins and Kwang Sik Kim for providing hBMECs, Scott Stibitz for the ΔLF/EF, ΔLF, and ΔEF mutant strains, Stephen Leppla for the purified PA and LF, and Mohammad Ebrahimi-Fardooee for performing quantification of ZO-1 fluorescence. The histopathologic analysis was performed at the University of California San Diego Histopathology Core Facility, Nissi Varki, director.

This work was supported by grant RO1 NS051247 from the NIH/NINDS to K.S.D.

REFERENCES

1. **Abramova, F. A., L. M. Grinberg, O. V. Yampolskaya, and D. H. Walker.** 1993. Pathology of inhalational anthrax in 42 cases from the Sverdlovsk outbreak of 1979. Proc. Natl. Acad. Sci. U. S. A. **90:**2291–2294.
2. **Agrawal, A., et al.** 2003. Impairment of dendritic cells and adaptive immunity by anthrax lethal toxin. Nature **424:**329–334.
3. **Ballabh, P., A. Braun, and M. Nedergaard.** 2004. The blood-brain barrier: an overview: structure, regulation, and clinical implications. Neurobiol. Dis. **16:**1–13.
4. **Bardwell, A. J., M. Abdollahi, and L. Bardwell.** 2004. Anthrax lethal factor-cleavage products of MAPK (mitogen-activated protein kinase) kinases exhibit reduced binding to their cognate MAPKs. Biochem. J. **378:**569–577.
5. **Beall, F. A., and F. G. Dalldorf.** 1966. The pathogenesis of the lethal effect of anthrax toxin in the rat. J. Infect. Dis. **116:**377–389.
6. **Betz, A. L.** 1985. Epithelial properties of brain capillary endothelium. Fed. Proc. **44:**2614–2615.
7. **Betz, A. L.** 1992. An overview of the multiple functions of the blood-brain barrier. NIDA Res. Monogr. **120:**54–72.
8. **Coombes, B. K., B. Chiu, I. W. Fong, and J. B. Mahony.** 2002. *Chlamydia pneumoniae* infection of endothelial cells induces transcriptional activation of platelet-derived growth factor-B: a potential link to intimal thickening in a rabbit model of atherosclerosis. J. Infect. Dis. **185:**1621–1630.
9. **Dalldorf, F. G., and F. A. Beall.** 1967. Capillary thrombosis as a cause of death in experimental anthrax. Arch. Pathol. **83:**154–161.
10. **Dejana, E.** 2004. Endothelial cell-cell junctions: happy together. Nat. Rev. Mol. Cell Biol. **5:**261–270.
11. **Deretic, V., and B. Levine.** 2009. Autophagy, immunity, and microbial adaptations. Cell Host Microbe **5:**527–549.
12. **Dixon, T. C., M. Meselson, J. Guillemin, and P. C. Hanna.** 1999. Anthrax. N. Engl. J. Med. **341:**815–826.
13. **Doran, K. S., et al.** 2005. Blood-brain barrier invasion by group B *Streptococcus* depends upon proper cell-surface anchoring of lipoteichoic acid. J. Clin. Invest. **115:**2499–2507.
14. **Doran, K. S., G. Y. Liu, and V. Nizet.** 2003. Group B streptococcal beta-hemolysin/cytolysin activates neutrophil signaling pathways in brain endothelium and contributes to development of meningitis. J. Clin. Invest. **112:**736–744.
15. **Duesbery, N. S., et al.** 1998. Proteolytic inactivation of MAP-kinase-kinase by anthrax lethal factor. Science **280:**734–737.
16. **Ebrahimi, C. M., et al.** 2009. Penetration of the blood-brain barrier by *Bacillus anthracis* requires the pXO1-encoded BslA protein. J. Bacteriol. **191:**7165–7173.
17. **Evans, D. J., I. A. Maltseva, J. Wu, and S. M. Fleiszig.** 2002. *Pseudomonas aeruginosa* internalization by corneal epithelial cells involves MEK and ERK signal transduction proteins. FEMS Microbiol. Lett. **213:**73–79.
18. **Firoved, A. M., et al.** 2005. *Bacillus anthracis* edema toxin causes extensive tissue lesions and rapid lethality in mice. Am. J. Pathol. **167:**1309–1320.
19. **Fritz, D. L., et al.** 1995. Pathology of experimental inhalation anthrax in the rhesus monkey. Lab. Invest. **73:**691–702.
20. **Giaever, I., and C. R. Keese.** 1991. Micromotion of mammalian cells measured electrically. Proc. Natl. Acad. Sci. U. S. A. **88:**7896–7900.
21. **Giaever, I., and C. R. Keese.** 1984. Monitoring fibroblast behavior in tissue culture with an applied electric field. Proc. Natl. Acad. Sci. U. S. A. **81:**3761–3764.
22. **Giaever, I., and C. R. Keese.** 1993. A morphological biosensor for mammalian cells. Nature **366:**591–592.
23. **Guichard, A., et al.** 2010. Anthrax toxins cooperatively inhibit endocytic recycling by the Rab11/Sec15 exocyst. Nature **467:**854–858.
24. **Gutierrez, M. G., et al.** 2007. Protective role of autophagy against *Vibrio cholerae* cytolysin, a pore-forming toxin from *V. cholerae.* Proc. Natl. Acad. Sci. U. S. A. **104:**1829–1834.
25. **Hoover, D. L., et al.** 1994. Anthrax edema toxin differentially regulates lipopolysaccharide-induced monocyte production of tumor necrosis factor alpha and interleukin-6 by increasing intracellular cyclic AMP. Infect. Immun. **62:**4432–4439.
26. **Iwai-Kanai, E., et al.** 2008. A method to measure cardiac autophagic flux in vivo. Autophagy **4:**322–329.
27. **Janes, B. K., and S. Stibitz.** 2006. Routine markerless gene replacement in *Bacillus anthracis.* Infect. Immun. **74:**1949–1953.
28. **Kabeya, Y., et al.** 2004. LC3, GABARAP and GATE16 localize to autophagosomal membrane depending on form-II formation. J. Cell Sci. **117:**2805–2812.
29. **Kim, K. S.** 2008. Mechanisms of microbial traversal of the blood-brain barrier. Nat. Rev. Microbiol. **6:**625–634.
30. **Kim, K. S.** 2002. Strategy of *Escherichia coli* for crossing the blood-brain barrier. J. Infect. Dis. **186**(Suppl. 2)**:**S220–S224.
31. **Kim, S. O., et al.** 2003. Sensitizing anthrax lethal toxin-resistant macrophages to lethal toxin-induced killing by tumor necrosis factor-alpha. J. Biol. Chem. **278:**7413–7421.
32. **Kugler, S., et al.** 2007. Pertussis toxin transiently affects barrier integrity, organelle organization and transmigration of monocytes in a human brain microvascular endothelial cell barrier model. Cell. Microbiol. **9:**619–632.
33. **Lanska, D. J.** 2002. Anthrax meningoencephalitis. Neurology **59:**327–334.
34. **Lehmann, M., D. Noack, M. Wood, M. Perego, and U. G. Knaus.** 2009. Lung epithelial injury by *B. anthracis* lethal toxin is caused by MKK-dependent loss of cytoskeletal integrity. PLoS One **4:**e4755.
35. **Lembo, A., et al.** 2010. Regulation of CovR expression in group B *Streptococcus* impacts blood-brain barrier penetration. Mol. Microbiol. **77:**431–443.
36. **Leppla, S. H.** 1982. Anthrax toxin edema factor: a bacterial adenylate cyclase that increases cyclic AMP concentrations of eukaryotic cells. Proc. Natl. Acad. Sci. U. S. A. **79:**3162–3166.
37. **Leppla, S. H.** 1984. *Bacillus anthracis* calmodulin-dependent adenylate cyclase: chemical and enzymatic properties and interactions with eucaryotic cells. Adv. Cyclic Nucleotide Protein Phosphorylation Res. **17:**189–198.
38. **Lo, C. M., C. R. Keese, and I. Giaever.** 1995. Impedance analysis of MDCK cells measured by electric cell-substrate impedance sensing. Biophys. J. **69:**2800–2807.
39. **Moayeri, M., D. Haines, H. A. Young, and S. H. Leppla.** 2003. *Bacillus anthracis* lethal toxin induces TNF-alpha-independent hypoxia-mediated toxicity in mice. J. Clin. Invest. **112:**670–682.
40. **Moayeri, M., and S. H. Leppla.** 2009. Cellular and systemic effects of anthrax lethal toxin and edema toxin. Mol. Aspects Med. **30:**439–455.
41. **Moayeri, M., and S. H. Leppla.** 2004. The roles of anthrax toxin in pathogenesis. Curr. Opin. Microbiol. **7:**19–24.
42. **Mock, M., and A. Fouet.** 2001. Anthrax. Annu. Rev. Microbiol. **55:**647–671.
43. **Mourez, M.** 2004. Anthrax toxins. Rev. Physiol. Biochem. Pharmacol. **152:**135–164.
44. **Nizet, V., et al.** 1997. Invasion of brain microvascular endothelial cells by group B streptococci. Infect. Immun. **65:**5074–5081.
45. **O'Brien, J., A. Friedlander, T. Dreier, J. Ezzell, and S. Leppla.** 1985. Effects of anthrax toxin components on human neutrophils. Infect. Immun. **47:**306–310.
46. **Pentecost, M., G. Otto, J. A. Theriot, and M. R. Amieva.** 2006. *Listeria monocytogenes* invades the epithelial junctions at sites of cell extrusion. PLoS Pathog. **2:**29–40.
47. **Pezard, C., P. Berche, and M. Mock.** 1991. Contribution of individual toxin components to virulence of *Bacillus anthracis.* Infect. Immun. **59:**3472–3477.
48. **Py, B. F., M. M. Lipinski, and J. Yuan.** 2007. Autophagy limits *Listeria monocytogenes* intracellular growth in the early phase of primary infection. Autophagy **3:**117–125.
49. **Rejman, J., S. Di Gioia, A. Bragonzi, and M. Conese.** 2007. *Pseudomonas aeruginosa* infection destroys the barrier function of lung epithelium and enhances polyplex-mediated transfection. Hum. Gene Ther. **18:**642–652.
50. **Ring, A., J. N. Weiser, and E. I. Tuomanen.** 1998. Pneumococcal trafficking across the blood-brain barrier. Molecular analysis of a novel bidirectional pathway. J. Clin. Invest. **102:**347–360.
51. **Sheen, T. R., et al.** 2010. Penetration of the blood-brain barrier by *Staphy-*

lococcus aureus: contribution of membrane-anchored lipoteichoic acid. J. Mol. Med. **88:**633–639.
52. **Soong, G., D. Parker, M. Magargee, and A. S. Prince.** 2008. The type III toxins of *Pseudomonas aeruginosa* disrupt epithelial barrier function. J. Bacteriol. **190:**2814–2821.
53. **Stins, M. F., F. Gilles, and K. S. Kim.** 1997. Selective expression of adhesion molecules on human brain microvascular endothelial cells. J. Neuroimmunol. **76:**81–90.
54. **Stins, M. F., N. V. Prasadarao, J. Zhou, M. Arditi, and K. S. Kim.** 1997. Bovine brain microvascular endothelial cells transfected with SV40-large T antigen: development of an immortalized cell line to study pathophysiology of CNS disease. In Vitro Cell. Dev. Biol. Anim. **33:**243–247.
55. **Tan, Y. K., et al.** 2009. Induction of autophagy by anthrax lethal toxin. Biochem. Biophys. Res. Commun. **379:**293–297.
56. **Tang, P., C. L. Sutherland, M. R. Gold, and B. B. Finlay.** 1998. *Listeria monocytogenes* invasion of epithelial cells requires the MEK-1/ERK-2 mitogen-activated protein kinase pathway. Infect. Immun. **66:**1106–1112.
57. **Terebiznik, M. R., et al.** 2009. Effect of *Helicobacter pylori's* vacuolating cytotoxin on the autophagy pathway in gastric epithelial cells. Autophagy **5:**370–379.
58. **van Sorge, N. M., et al.** 2008. Anthrax toxins inhibit neutrophil signaling pathways in brain endothelium and contribute to the pathogenesis of meningitis. PLoS One **3:**e2964.
59. **Vitale, G., L. Bernardi, G. Napolitani, M. Mock, and C. Montecucco.** 2000. Susceptibility of mitogen-activated protein kinase kinase family members to proteolysis by anthrax lethal factor. Biochem. J. **352**(Pt 3)**:**739–745.
60. **Warfel, J. M., A. D. Steele, and F. D'Agnillo.** 2005. Anthrax lethal toxin induces endothelial barrier dysfunction. Am. J. Pathol. **166:**1871–1881.
61. **Webster, J. I., et al.** 2003. Anthrax lethal factor represses glucocorticoid and progesterone receptor activity. Proc. Natl. Acad. Sci. U. S. A. **100:**5706–5711.

Editor: J. B. Bliska